ACS OMEGA

Open Access

http://pubs.acs.org/journal/acsodf

Article

Prognostic Prediction and Immune Microenvironment Characterization in Uveal Melanoma: A Novel Mitochondrial Metabolism-Related Gene Signature

Wei-Jun Cai, Ru-Ru Chen, Zi-Bin Liu, Jian Lai, Li-Jie Hou, and Rui Zhang*

Cite This: *ACS Omega* 2024, 9, 43034−43045

Read Online

ACCESS | Metrics & More | Article Recommendations | Supporting Information

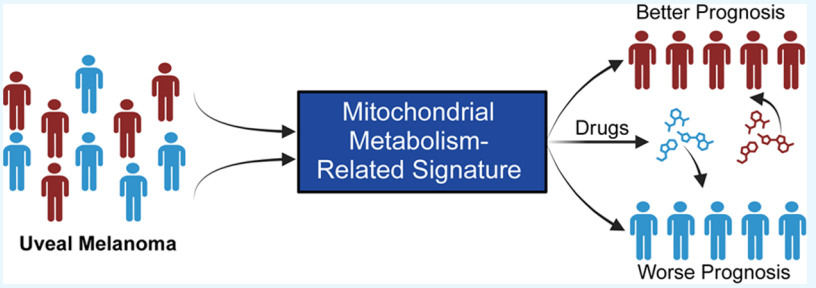

ABSTRACT: Uveal Melanoma (UM), a highly aggressive and metastatic intraocular cancer with a strong propensity for liver metastasis, presents limited therapeutic alternatives and unfavorable survival outcomes. Despite its low incidence, the underlying mechanisms of UM pathogenesis and the precise role of mitochondrial metabolism in UM remain inadequately understood. Utilizing Cox proportional hazards regression analysis was used to assess prognostic relevance, and consensus clustering was employed for molecular subtyping. A risk signature was constructed using Least Absolute Shrinkage and Selection Operator (LASSO) Cox regression. We further conducted comparative analyses on clinicopathological characteristics, somatic mutation profiles, drug sensitivity, gene expression patterns, and tumor microenvironment features across different molecular subtypes. Moreover, a nomogram was developed and evaluated. Among 1234 mitochondria metabolism-related genes (MMRGs), 343 were identified as significantly associated with the prognosis of UM. These prognosis-associated MMRGs facilitated the classification of UM into two distinct molecular subtypes, which displayed notable differences in prognosis and pathological staging. Furthermore, an index termed the MMRGs-derived index (MMI) was derived from eight MMRGs, serving as a quantitative measure for poor prognosis risk in UM. MMI demonstrated significant associations with clinicopathological characteristics, somatic mutations, drug responsiveness, and the tumor microenvironment, where higher MMI levels corresponded to worse prognosis, advanced pathological stages, and increased immune cell infiltration. The nomogram built upon MMI provided a potential tool for clinical prognosis assessment in UM patients. This study demonstrated the potential value of MMRGs in predicting prognosis and molecular stratification within UM; however, additional clinical and basic research is warranted to validate their applicability and elucidate the related mechanisms.

INTRODUCTION

Uveal Melanoma (UM), a rare yet highly aggressive malignant intraocular tumor in adults, originates from melanocytes within the choroid, ciliary body, and iris tissues.[1−4] Despite an annual global incidence rate of 5−6 cases per million individuals, UM prevalence significantly escalates among Caucasians and populations residing in higher latitudes; for instance, an average of 4.3 new cases per million population annually was reported in the United States.[1−3] UM is notorious for its local destructiveness and high metastatic potential, predominantly to the liver, leading to poor prognosis with over 40% of patients succumbing to systemic disease within a decade postdiagnosis, and median survival time dwindling to less than one year following metastasis.[4,5] While primary UM can be managed using a range of modalities such as surgery and radiotherapy including episcleral plaque brachytherapy, treatment options are limited for metastatic UM patients, who typically have a median overall survival (OS) of merely 6−12 months and low long-term survival rates.[6,7] Hence, it is imperative to delve deeper into the pathogenesis of UM and explore novel systemic therapeutic approaches to enhance the prognosis for these patients.

Received: July 7, 2024
Revised: September 25, 2024
Accepted: September 30, 2024
Published: October 10, 2024

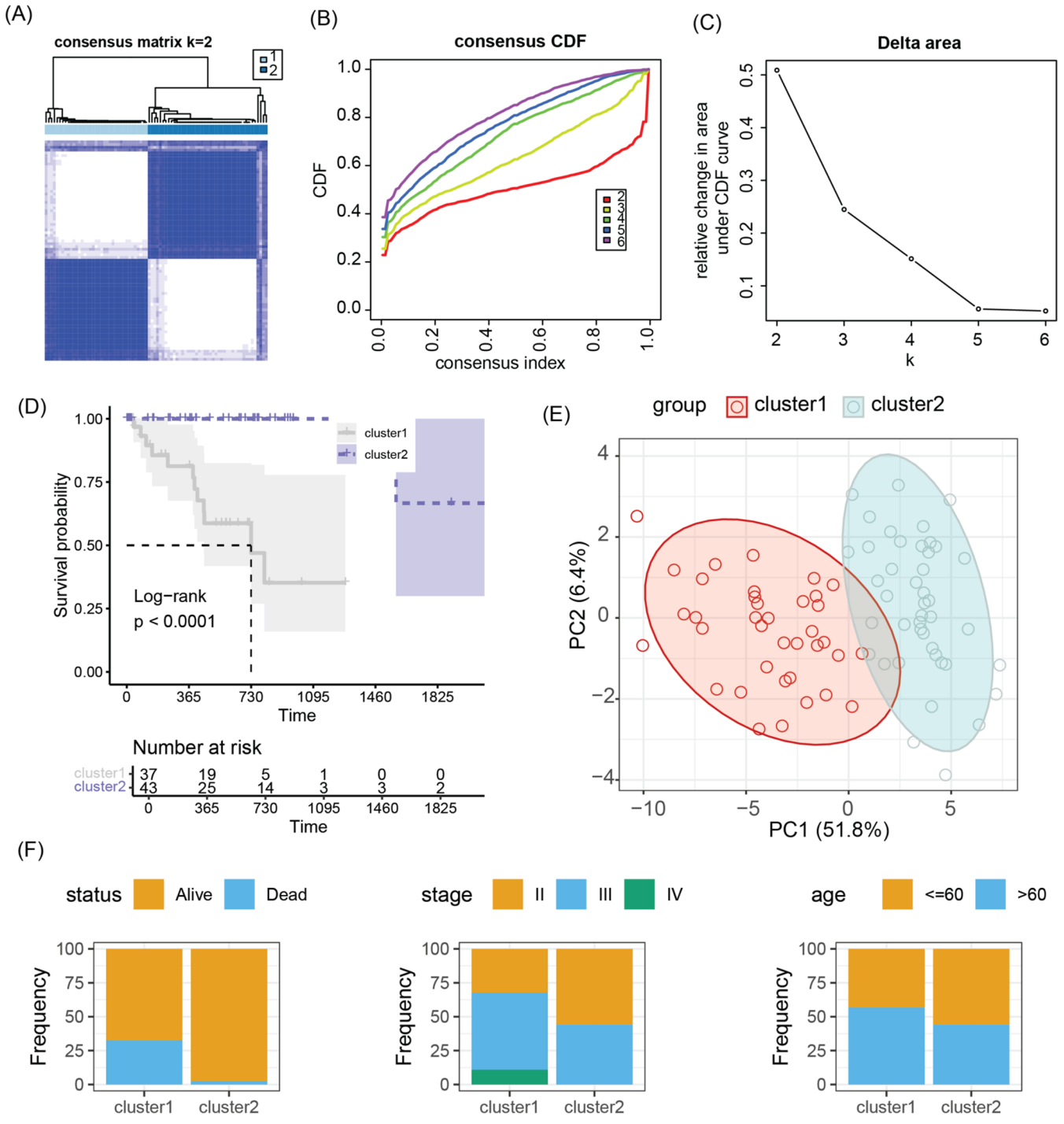

Figure 1. Molecular subtyping of TCGA-UVM cohort based on prognosis-related MMRGs. (A) Consensus matrix heatmap ($k = 2$) illustrating the probability that two patients belong to the same cluster within the TCGA-UVM samples, as determined by prognosis-related MMRGs. (B) Consensus Cumulative Distribution Function (CDF) plot. (C) Delta area plot in consensus clustering. (D) Kaplan−Meier survival curves and Log-rank test for UVM molecular subtypes derived from MMRGs. (E) Principal Component Analysis (PCA) based on prognosis-related MMRGs. (F) Comparisons of status, stage, and age between UVM molecular subtypes derived from MMRGs.

Mitochondria, central to cellular energy metabolism, have been implicated in the etiology and progression of various cancers. Studies demonstrated that metabolic reprogramming of mitochondria in tumor cells played a pivotal role in sustaining cancer cell proliferation, invasiveness, and drug resistance.[8−10] However, the influence of mitochondrial metabolism-related genes (MMRGs) on the prognosis of Uveal Melanoma, the most common primary intraocular malignancy in adults, remains inadequately explored. Although previous research has constructed prognostic models based on mitochondrial metabolic gene expression profiles in other types of tumors,[11−13] a comprehensive elucidation of the unique pathophysiological characteristics of UM and its underlying molecular mechanisms within the context of mitochondrial metabolism is still lacking.

https://doi.org/10.1021/acsomega.4c06294
ACS Omega 2024, 9, 43034−43045

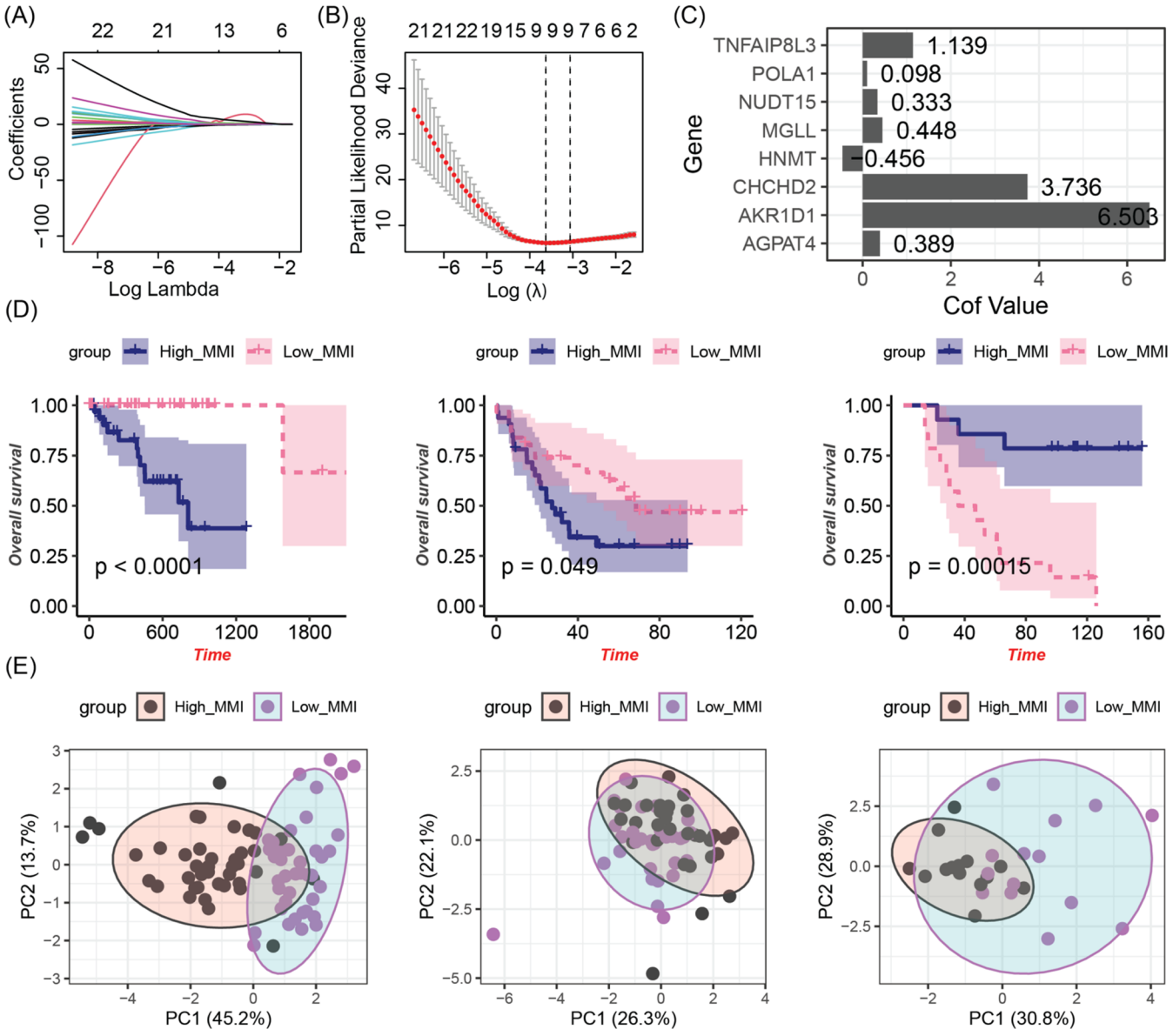

Figure 2. Construction of the UVM risk signature MMI based on MMRGs. (A, B) Lasso Cox regression used to select eight MMRGs for constructing the MMI feature in UVM. (C) The eight MMRGs composing the MMI and their corresponding coefficients. (D) Survival analysis comparing High_MMI and Low_MMI groups across TCGA-UVM, GSE84976, and GSE22138 cohorts. (E) PCA based on the eight MMRGs in TCGA-UVM, GSE84976, and GSE22138 data sets.

This study employed bioinformatics analysis methods to investigate the association between MMRGs and prognosis in UM, further utilizing consensus clustering for molecular subtyping. A MMRGs-derived index (MMI) was constructed using Least Absolute Shrinkage and Selection Operator (LASSO) regression, followed by functional enrichment analyses, correlations with clinical characteristics, immune infiltration assessments, and drug sensitivity evaluations. Our findings provided unique insights into the pivotal roles of MMRGs in the development and prognosis of UM, substantiating whether MMRGs can serve as viable prognostic biomarkers and potential therapeutic targets for UM patients.

MATERIALS AND METHODS

Data Retrieval and Preprocessing. We downloaded data from 80 UM patients in the TCGA-UVM project from The Cancer Genome Atlas (TCGA) Genomic Data Commons (GDC; https://portal.gdc.cancer.gov/), encompassing gene expression profiles, somatic mutations, and corresponding clinical-pathological characteristics. To augment and contrast our analysis, we also retrieved transcriptomic data sets and associated clinical information data sets from two independent cohorts—GSE84976 and GSE22138—via the Gene Expression Omnibus (GEO, https://www.ncbi.nlm.nih.gov/gds/) database. The GSE84976 cohort comprised data for 28 UM cases, while the GSE22138 cohort contained 63 UM cases. A total of 1234 MMRGs was obtained from the MSigDB database (Supporting Information: Table S1).

Consensus Clustering Analysis. Univariate Cox regression analysis was applied to evaluate the prognostic relevance of MMRGs with respect to UM and selected those MMRGs with $p < 0.05$ for consensus clustering analysis. Leveraging the ConsensusClusterPlus package,[14] we performed clustering using the partitioning around medoids method and the

https://doi.org/10.1021/acsomega.4c06294
ACS Omega 2024, 9, 43034−43045

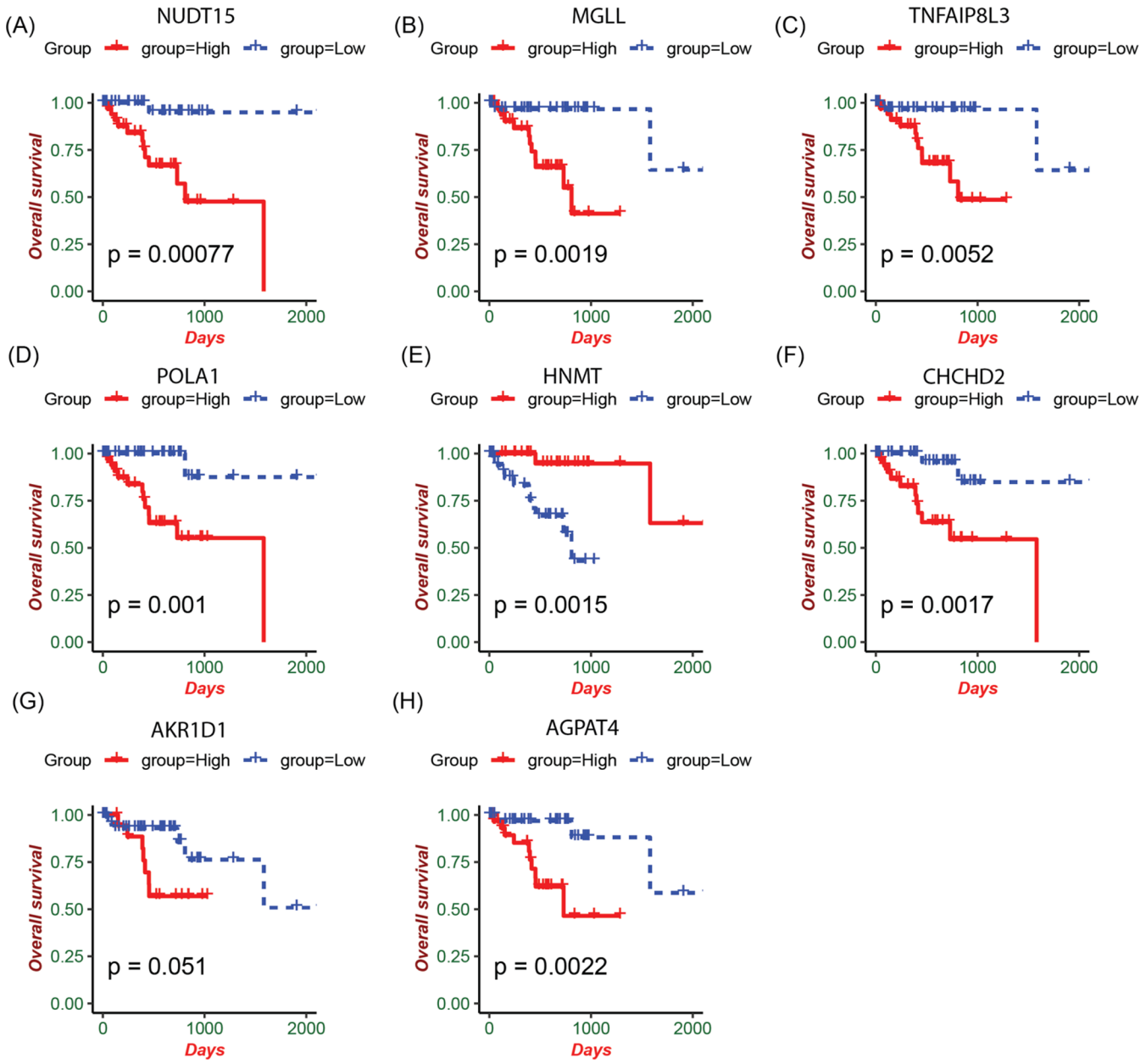

Figure 3. Kaplan−Meier survival analyses of genes composing the MMI. (A−H) Patients in the TCGA-UVM cohort were dichotomized into high and low expression groups based on median expression levels of NUDT15, MGLL, TNFAIP8L3, POLA1, HNMT, CHCHD2, AKR1D1, and AGPAT4, followed by survival analysis and Log-rank tests.

"pearson" distance function. Concurrently, survival analysis, principal component analysis, and intersubtype statistical analyses of clinical pathological features were conducted.

Construction of the MMRGs-Derived Risk Signature. Using the glmnet package,[15] we conducted LASSO Cox regression analysis to construct an MMI. The formula is as follows: MMI = $\sum(\beta i \times \text{expi})$. Here, βi represented the coefficient for gene i, and expi denoted the expression level of gene i. Based on the median value of MMI, we categorized patients from the TCGA-UVM, GSE84976, and GSE22138 cohorts into High_MMI and Low_MMI groups. Parallel principal component analysis (PCA) and survival analysis were then executed for these groups.

Somatic Mutation Analysis. The maftools package was employed to analyze and visualize somatic mutation data from the TCGA-UVM cohort.[16]

Immune Infiltration Analysis. The IOBR package was used for tumor microenvironment analysis, which incorporates multiple methods to assess immune infiltration in tumors, including CIBERSORT, EPIC, xCell, MCP-counter, ESTIMATE, TIMER, quanTIseq, and IPS, among others.[17]

Enrichment Analysis. Differential expression analysis was conducted using the edgeR package,[18] screening for differentially expressed genes (p = 0.05 and |log(fold change)| > 2). Gene ontology (GO) and Kyoto Encyclopedia of Genes and Genomes (KEGG) enrichment analyses were performed on these genes using the clusterProfiler package;[19] ID conversion was carried out with the bitr() function, while enrichGO() and enrichKEGG() functions were used for enrichment analysis, setting p-value cutoff at 0.05.

Drug Sensitivity Analysis. Drug sensitivity to a panel of 45 drugs, including Axitinib, Bexarotene, Bicalutamide,

https://doi.org/10.1021/acsomega.4c06294
ACS Omega 2024, 9, 43034−43045

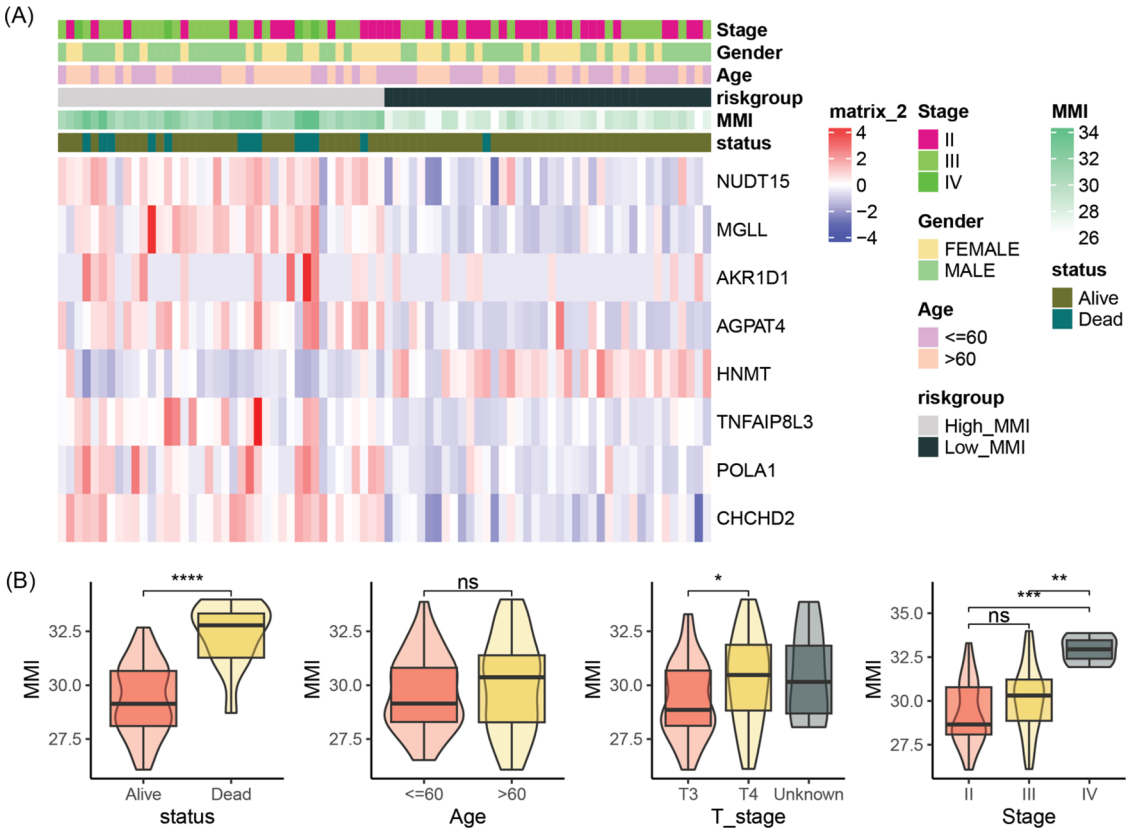

Figure 4. Correlation between MMI and clinicopathological characteristics in the TCGA-UVM cohort. (A) Heatmap showing the expression levels of MMI composing genes. (B) Comparison of MMI among different clinical pathological stages. *p < 0.05, **p < 0.01, ***p < 0.001, ****p < 0.0001.

Bleomycin, and Bortezomib, among others, was analyzed for patients in the TCGA-UVM cohort using the pRRophetic package.[20] The pRRopheticPredict() function was employed for sensitivity assessment, setting tissueType as "all" and applying batch correction through the ComBat method.

Nomogram Construction and Evaluation. Univariate and multivariate Cox regression analyses were performed to evaluate the prognostic significance of MMI and clinical pathological characteristics. Independent prognostic factors with p < 0.05 were selected to construct a nomogram predicting 1-, 2-, and 3-year overall survival rates for UM patients using the rms package. The performance of the nomogram was assessed through receiver operating characteristic (ROC) curve analysis, calibration curve analysis, and decision curve analysis using the rmda package.

Statistical Analysis. All statistical analyses and visualizations were conducted using R software (version 4.3.2). For intergroup differences, the Wilcoxon test was applied, with p < 0.05 considered statistically significant. Kaplan−Meier survival curves and Log-rank tests were executed using packages such as survival and survminer for survival analysis.

RESULTS

UM Molecular Subtyping Based on Prognostic-Related MMRGs. Univariate Cox regression analysis revealed that among the 1234 MMRGs, 343 were significantly associated with the prognosis of UM (p < 0.05, Supporting Information: Table S2). Using these prognostically relevant MMRGs, we conducted consensus clustering analysis (Figure 1A−C), which resulted in two distinct molecular subtypes of UM (cluster1 and cluster2). These subtypes showed significant differences in prognosis, with cluster1 having a poorer outcome compared to cluster2 (p < 0.0001, Figure 1D). Principal component analysis demonstrated a clear separation between cluster1 and cluster2 (Figure 1E), suggesting that the prognostic-related MMRGs effectively distinguish UM patients with different outcomes. Cluster1, with a worse prognosis, was characterized by a higher proportion of deaths, a greater percentage of advanced-stage cases, and a larger number of elderly patients compared to cluster2 (Figure 1F).

MMRG-Derived Index. To explore the value of MMRGs in UM prognosis risk assessment, we further selected 36 prognostically related MMRGs with p < 0.001 for LASSO Cox regression analysis (Figure 2A,B). This resulted in an eight-gene risk signature (Figure 2C), formulated as follows: MMI = 1.139 × TNFAIP8L3 + 0.098 × POLA1 + 0.333 × NUDT15 + 0.448 × MGLL − 0.456 × HNMT + 3.736 × CHCHD2 + 6.503 × AKR1D1 + 0.389 × AGPAT4. According to the median value of MMI, patients from the TCGA-UVM, GSE84976, and GSE22138 cohorts were categorized into High_MMI and Low_MMI groups. Survival analysis indicated that UM patients in the High_MMI group had a poorer prognosis than those in the Low_MMI group (Figure 2D). The PCA plots based on the MMI constituting genes are displayed in Figure 2E, where high expression of HNMT is indicative of a favorable prognosis, while elevated expression of other genes predicts a poor prognosis (Figure 3).

Association of MMI with Clinical Relevance. Figure 4A presented a heatmap illustrating the expression levels of the MMI constituting genes, showing that in comparison to the

https://doi.org/10.1021/acsomega.4c06294
ACS Omega 2024, 9, 43034−43045

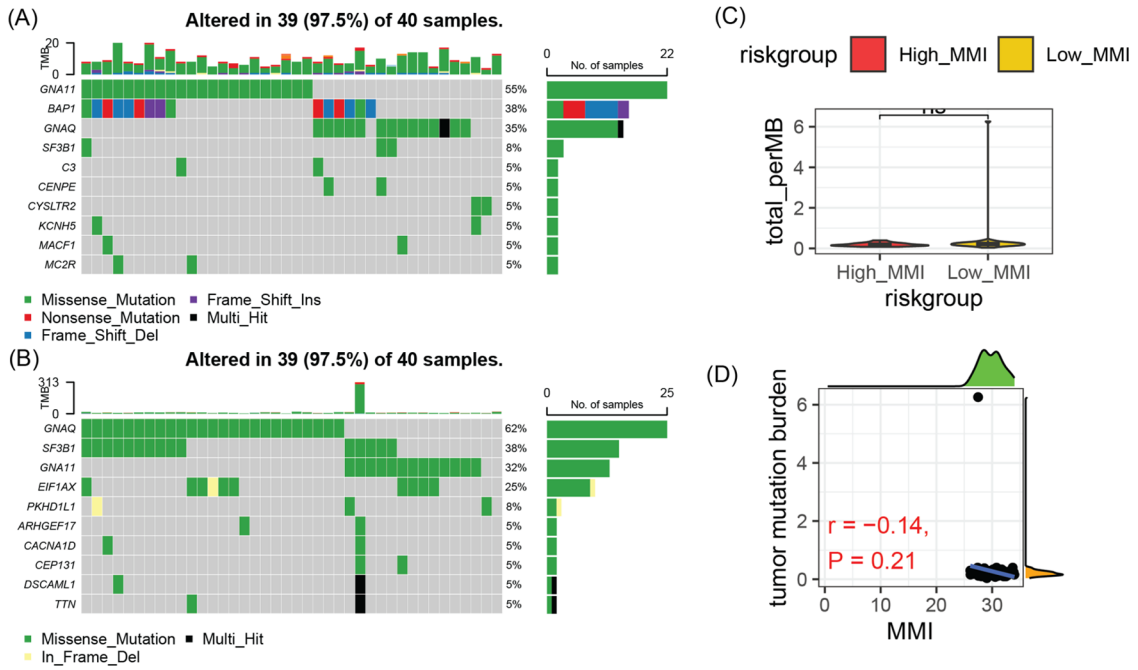

Figure 5. Association between MMI and somatic mutations in the TCGA-UVM cohort. (A) Oncoplot showing the top 10 most frequently mutated genes in High_MMI patients. (B) Oncoplot displaying the top 10 most frequently mutated genes in Low_MMI patients. (C) Comparison of TMB between High_MMI and Low_MMI groups. (D) Scatter plot depicting the correlation between MMI and TMB. ns, not significant.

High_MMI group, the Low_MMI group has higher expression of HNMT and lower expression of the other genes. Moreover, the High_MMI group had more deceased patients and advanced-stage cases. Furthermore, when comparing MMI across different clinical pathological stages, it was observed that deceased or advanced stage patients generally exhibited higher MMI values compared to their respective counterparts in other staging categories (Figure 4B).

Correlation of MMI with Somatic Mutations. In the High_MMI group, the top 10 most frequently mutated genes were GNA11, BAP1, GNAQ, SF3B1, C3, CENPE, CYSLTR2, KCNH5, MACF1, and MC2R (Figure 5A), whereas in the Low_MMI group, they were GNAQ, SF3B1, GNA11, EIF1AX, PKHD1L1, ARHGEF17, CACNA1D, CEP131, DSCAML1, and TTN (Figure 5B). However, there was no significant difference in Tumor Mutation Burden (TMB) between the High_MMI and Low_MMI groups, nor was there a significant correlation between MMI and TMB (Figure 5C,D).

Biological Functions and Pathways Related to MMI. Differential expression analysis revealed 834 differentially expressed genes between the High_MMI and Low_MMI groups ($p < 0.05$, |log(fold change)| > 2). KEGG enrichment analysis showed that these genes were enriched in pathways related to ligand−receptor interactions and immune regulation, such as the T cell receptor signaling pathway, chemokine signaling pathway, antigen processing and presentation, and T cell differentiation (Figure 6A). GO enrichment analysis indicated that these genes were also enriched in biological processes like regulation of cytokine production, pyroptosis, cell killing, and mononuclear cell differentiation (Figure 6B).

Association between MMI and Drug Sensitivity. Upon analyzing drug sensitivity for 45 drugs in the TCGA-UVM cohort, we found that compared to the High_MMI group, patients in the Low_MMI group exhibited higher sensitivity to 21 drugs, including vinorelbine, vinblastine, and thapsigargin, while showing lower sensitivity to 6 drugs such as temsirolimus, rapamycin, and nilotinib (Figure 7A). Correlation analysis demonstrated that MMI was associated with the sensitivity to most drugs, and except for HNMT, the expression levels of other constituting genes of MMI had correlations with drug sensitivity that were largely consistent with those of MMI itself (Figure 7B).

Relationship between MMI and Tumor Microenvironment. To explore the relationship between MMI and the tumor microenvironment, we utilized eight algorithms for analysis. The results showed that MMI was significantly correlated with infiltrating levels of T cells, NK cells, macrophages, neutrophils, fibroblasts, etc., with distinct differences observed between the High_MMI and Low_MMI groups (Figure 8A). Compared to the High_MMI group, the Low_MMI group had lower StromalScore, ImmuneScore, ESTIMATEScore, and higher Tumor purity (Figure 8B). Furthermore, the Low_MMI group displayed lower MGC_IPS, EC_IPS, AZ_IPS, and higher SC_IPS, CP_IPS (Figure 8C). These findings suggested a significant correlation between MMI and the tumor microenvironment.

Nomogram Based on MMI. Through univariate and multivariate Cox analyses, we identified MMI as a potential independent factor for predicting OS in UM patients (Table 1). To optimize clinical application based on MMI, we constructed a nomogram to predict 1-year, 2-year, and 3-year OS for UM patients (Figure 9A). The calibration curve for the nomogram in predicting the 1-year and 2-year OS of UM patients is shown in Figure 9B. Additionally, ROC analysis revealed that the Area Under the Curve (AUC) values for predicting 1-year, 2-year, and 3-year OS using the nomogram were 0.957, 0.985, and 0.98, respectively (Figure 9C). Lastly, through decision curve analysis, we found that the nomogram outperformed other prognostic factors in terms of standardized net benefit for predicting 1-year OS in UM patients (Figure 9D).

https://doi.org/10.1021/acsomega.4c06294
ACS Omega 2024, 9, 43034−43045

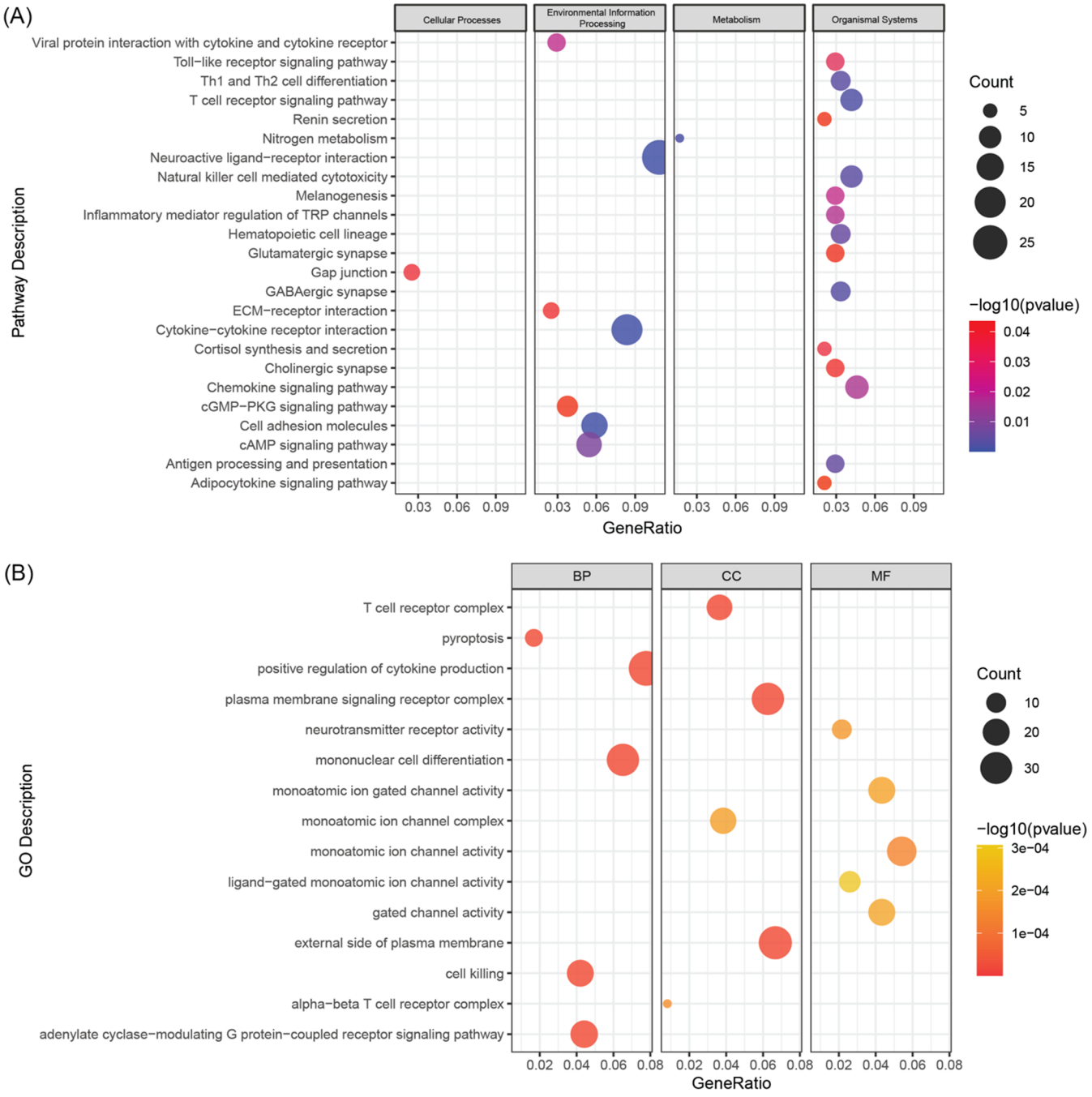

Figure 6. Associations between MMI and biological functions/pathways in the TCGA-UVM cohort. (A) KEGG enrichment analysis of differentially expressed genes between High_MMI and Low_MMI groups. (B) GO enrichment analysis of differentially expressed genes between High_MMI and Low_MMI groups.

DISCUSSION

In the present study, 343 MMRGs were found to be significantly associated with the prognosis of UM, and molecular subtyping based on these genes led to the identification of two distinct subtypes with significantly different prognoses. Further, an index named MMI, constructed from eight MMRGs, was developed and demonstrated a strong predictive capacity for UM prognosis. MMI showed significant correlations with clinical-pathological characteristics, somatic mutation profiles, drug sensitivity, as well as the tumor microenvironment in UM patients. Moreover, a nomogram based on MMI effectively guided the prediction of clinical outcomes in UM. These findings suggested that MMRGs might serve as potential prognostic biomarkers for distinguishing different molecular subtypes of UM and contributed to predicting patients' clinical outcomes.

Among the MMRGs constituting MMI, TNFAIP8L3 has been demonstrated to activate the PI3K-AKT and MEK-ERK pathways, playing a critical role in regulating inflammation responses, immune homeostasis, and cancer development.[21,22] POLA1 and NUDT15 are pivotal in DNA replication and metabolic processes,[23,24] with aberrations in DNA metabolism being interconnected with mitochondrial dysfunction and carcinogenesis.[25,26] The HNMT gene encodes histamine *N*-

https://doi.org/10.1021/acsomega.4c06294
ACS Omega 2024, 9, 43034−43045

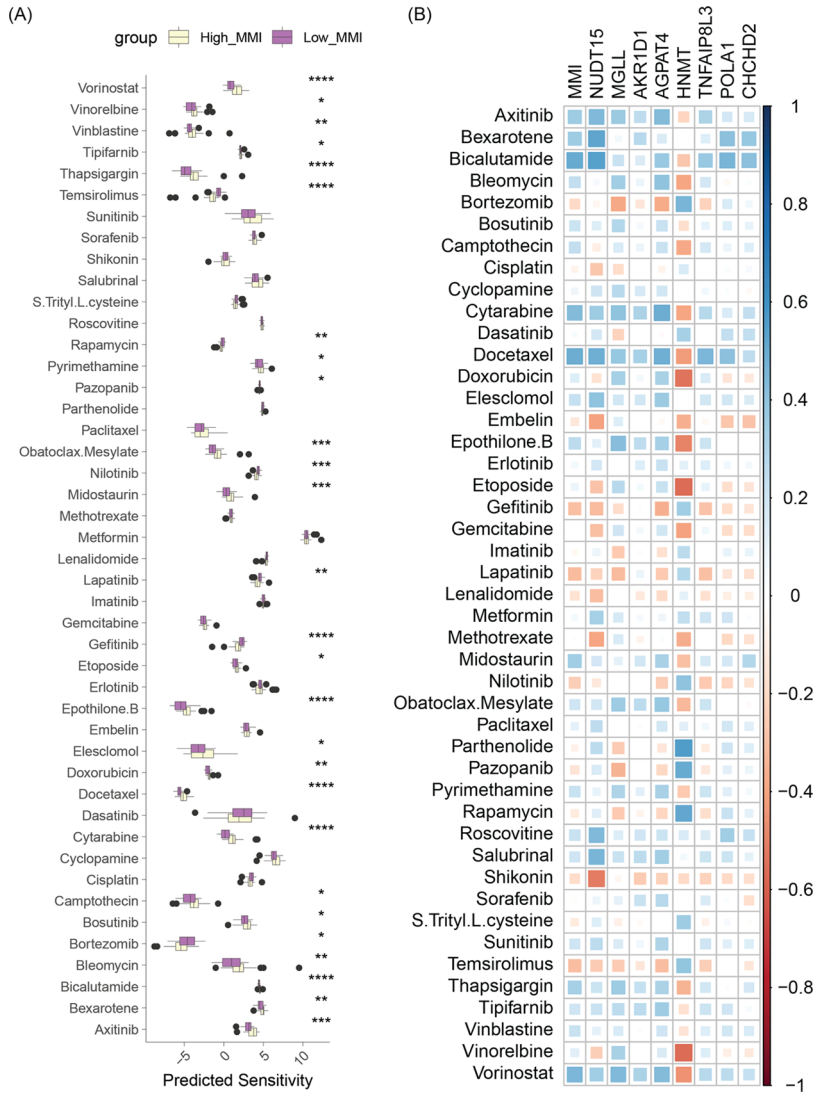

Figure 7. Relationship between MMI and drug sensitivity in the TCGA-UVM cohort. (A) Differences in drug sensitivity to 45 drugs between High_MMI and Low_MMI groups of UVM patients. (B) Heatmap representing correlations between MMI and its composing genes with sensitivity to 45 drugs. *$p < 0.05$, **$p < 0.01$, ***$p < 0.001$, ****$p < 0.0001$.

methyltransferase, which primarily converts histamine to *N*-methylhistamine; histamine modulates oxidative stress, inflammatory responses, and energy metabolism-related pathways, thereby influencing mitochondrial homeostasis and overall cellular metabolism.[27] HNMT affected the tumor microenvironment, including angiogenesis, cell proliferation, and apoptosis, by regulating histamine-mediated signaling.[28] CHCHD2, encoding a mitochondrial protein involved in the regulation of mitochondrial internal structure and function,[29] could potentially act as a molecular marker or therapeutic target in cancer progression by influencing mitochondrial oxidative phosphorylation processes and related energy metabolism pathways, thus promoting cancer cell proliferation, invasion, and migration.[30]

Aberrant lipid metabolism is a hallmark of tumor cells, with reprogramming of lipid metabolism, including within mitochondria, supporting tumor growth, invasion, and metastasis.[31] MGLL, AGPAT4, and AKR1D1 primarily participate in lipid metabolism and may serve as potential therapeutic targets through their involvement in lipid metabolic reprogramming in cancer treatment. Studies have shown that AKR1D1 can potentially influence cancer cell proliferation, migration, and invasiveness by affecting cholesterol metabolism and its downstream products, such as bile acids.[32,33] Additionally, the AGPAT4/LPA axis in colorectal cancer cells regulated p38/p65 signal-dependent macrophage polarization, T-cell activation, and colorectal cancer progression,[34] implicating AGPAT4 as a potential clinical therapeutic target.

A pivotal novel finding revealed a significant association between MMI and the extent of infiltration by various cell populations within UM tumors, encompassing T lymphocytes, natural killer cells, eosinophils, fibroblasts, as well as macrophages and mast cells. Research has shown that certain immune cells, such as macrophages, neutrophils, mast cells, and activated T cells, released extracellular enzymes, angiogenic factors, and chemokines with recruiting functions in the tumor microenvironment, processed which have been demonstrated to promote tumor growth.[35,36] Moreover, the distribution and activity of immune cells within the tumor were decisive for the efficacy of cancer immunotherapy.[37] Given this backdrop, we speculated that the aberrations in MMRGs might indirectly influence the responsiveness of UM patients to

https://doi.org/10.1021/acsomega.4c06294
ACS Omega 2024, 9, 43034−43045

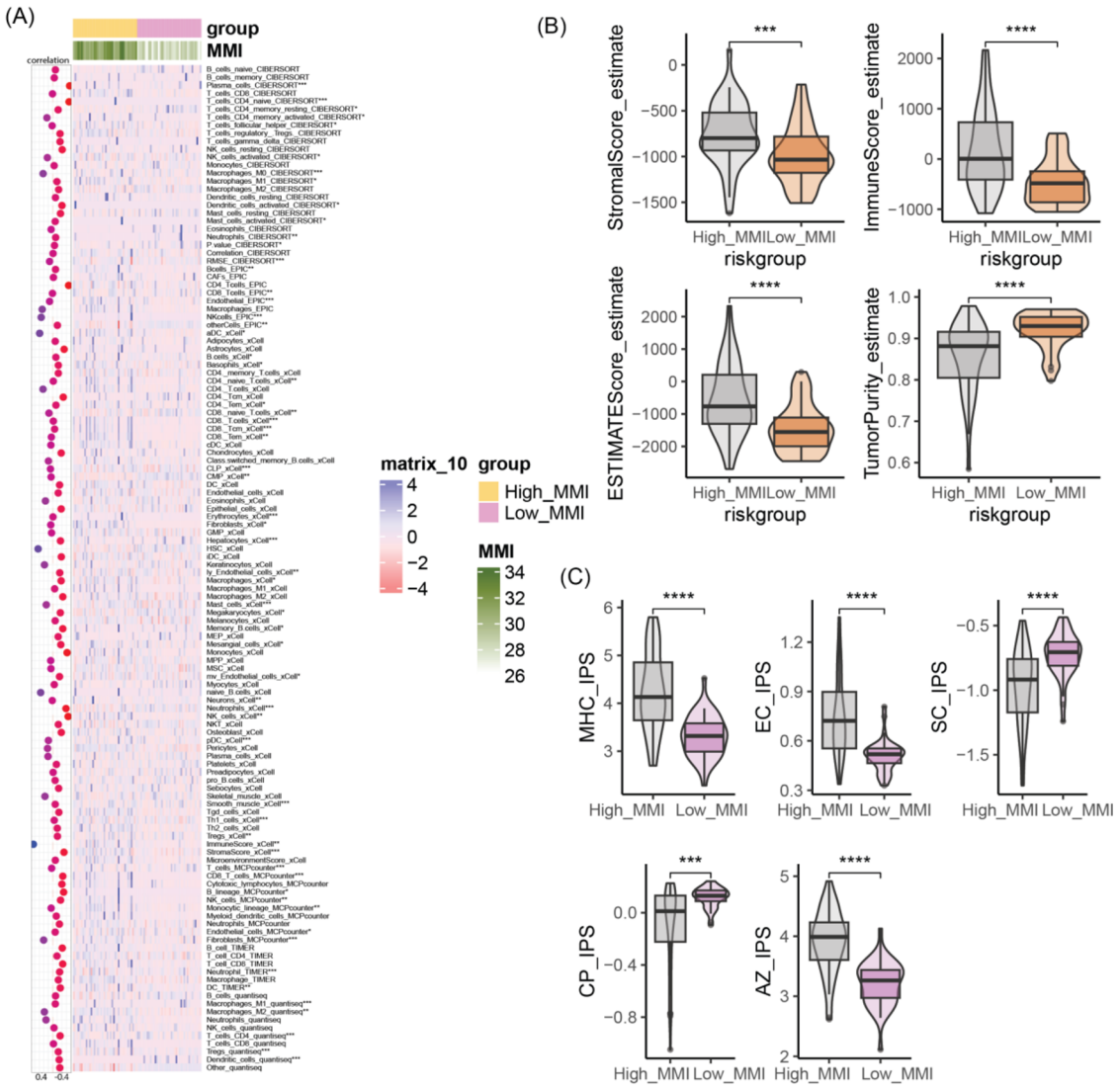

Figure 8. Association between MMI and tumor microenvironment in the TCGA-UVM cohort. (A) Comparison of tumor immune cell infiltration differences between High_MMI and Low_MMI groups. (B) Comparison of Stromalscore, ImmuneScore, ESTIMATEscore, and Tumor purity between High_MMI and Low_MMI groups. (C) Comparison of MHC_IPS, EC_IPS, SC_IPS, CP_IPS, AZ_IPS between High_MMI and Low_MMI groups. *$p < 0.05$, **$p < 0.01$, ***$p < 0.001$, ****$p < 0.0001$.

Table 1. Details Results of the Univariate and Multivariate Cox Regression Analyses

	univariate Cox				multivariate Cox			
characteristics	HR	lower.95	upper.95	*p*	HR	lower. 95	upper. 95	*p*
MMI	5.6	2.2	14	0.00023	5.67	1.7	18.89	0.005
age	6	1.3	28	0.023	5.99	0.41	86.9	0.19
stage	6.9	1.5	31	0.012	4.04	0.41	39.64	0.231
gender	0.3	0.066	1.4	0.13	0.46	0.06	3.4	0.443
T stage	4	0.84	19	0.081	1.76	0.07	45.89	0.733

immunotherapeutic interventions. Therefore, a thorough dissection of MMRG characteristics and their interplay with the functional mechanisms of infiltrating immune cells within tumors holds promise to provide new theoretical foundations for personalized treatment strategies in UM patients.

Despite our current research elucidating the potential utility of MMRGs in prognosis assessment for UM and successfully devising the risk assessment model MMI based on these genes, several limitations remain to be addressed. First, while the significant correlation between MMRGs and UM patient prognosis and the construction of MMI represent pioneering strides, it is imperative to validate its predictive accuracy and generalizability across different prospective cohorts and diverse patient subgroups in subsequent steps. Second, although this study has explored the relationship between MMI and disease progression in UM and tumor immune infiltration, the detailed molecular mechanisms by which mitochondrial metabolic dysfunction specifically operates in the initiation, development, and metastatic processes of UM require further investigation.

https://doi.org/10.1021/acsomega.4c06294
ACS Omega 2024, 9, 43034−43045

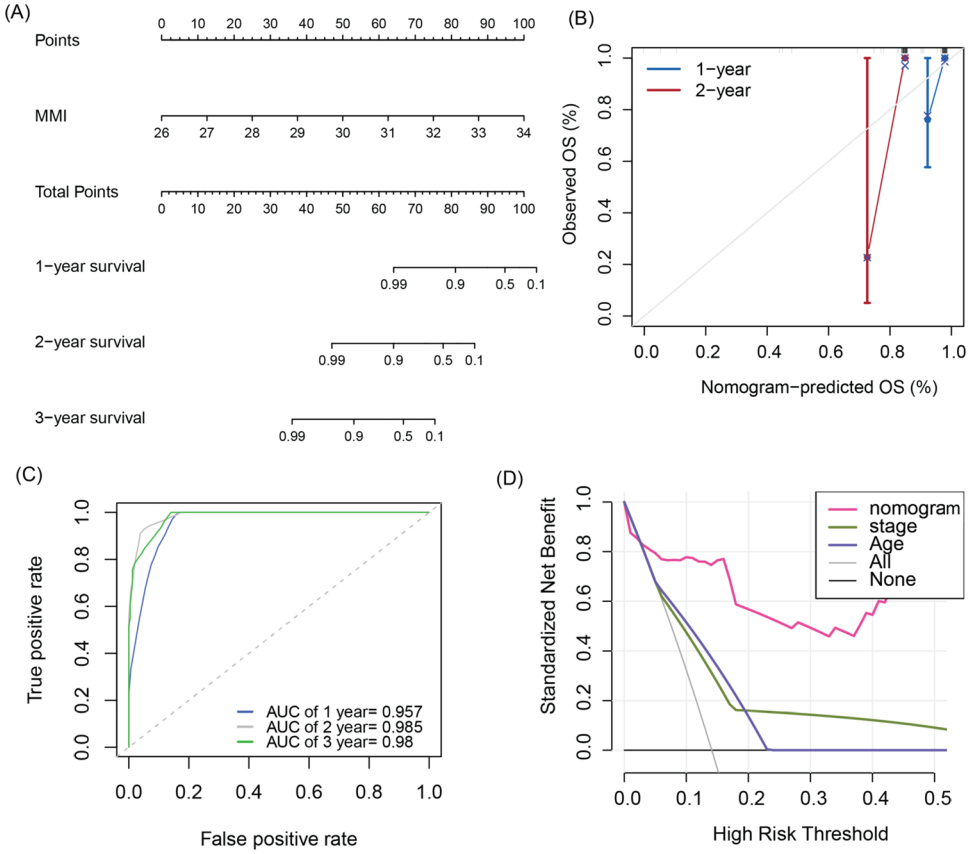

Figure 9. Development of a nomogram for UVM patient prognosis assessment based on MMI. (A) Nomogram model predicting 1-, 2-, and 3-year overall survival rates for UVM patients based on MMI. (B) Calibration curve analysis of nomogram-predicted 1- and 2-year overall survival rates. (C) ROC curve analysis of nomogram-predicted 1-, 2-, and 3-year overall survival rates. (D) Decision curve analysis of nomogram-predicted 1-year overall survival rate.

CONCLUSIONS

In summary, this study elucidated the prognostic relevance of MMRGs in UM, and substantiated the applicability of molecular subtyping based on MMRGs for prognosis assessment and therapeutic guidance in UM. Ultimately, a risk signature MMI was developed, comprising eight MMRGs, with an associated nomogram that can be utilized for clinical prognosis evaluation in UM patients. However, the validity of these models necessitates further validation through larger prospective clinical studies, and the underlying mechanisms by which MMRGs contribute to the progression of UM require additional experimental exploration.

ASSOCIATED CONTENT

Data Availability Statement

All data generated or analyzed during the present study are included in this published article or are available from the corresponding author on reasonable request.

Supporting Information

The Supporting Information is available free of charge at https://pubs.acs.org/doi/10.1021/acsomega.4c06294.

MMRGs obtained from the MSigDB database; detail results of univariate cox regression analysis of MMRGs in the TCGA-UVM cohort (PDF)

AUTHOR INFORMATION

Corresponding Author

Rui Zhang − *Department of Ophthalmology, Hangzhou TCM Hospital Affiliated to Zhejiang Chinese Medical University, Hangzhou, Zhejiang 310007, China*; orcid.org/0009-0001-2964-8586; Phone: +86 15867755372; Email: zhangrui_jk@163.com

Authors

Wei-Jun Cai − *National Clinical Research Center for Ocular Diseases, Eye Hospital, Wenzhou Medical University, Wenzhou, Zhejiang 325027, China*

Ru-Ru Chen − *National Clinical Research Center for Ocular Diseases, Eye Hospital, Wenzhou Medical University, Wenzhou, Zhejiang 325027, China*

Zi-Bin Liu − *Department of Ophthalmology, Hangzhou TCM Hospital Affiliated to Zhejiang Chinese Medical University, Hangzhou, Zhejiang 310007, China*

Jian Lai − *Department of Ophthalmology, Hangzhou TCM Hospital Affiliated to Zhejiang Chinese Medical University, Hangzhou, Zhejiang 310007, China*

Li-Jie Hou − *National Clinical Research Center for Ocular Diseases, Eye Hospital, Wenzhou Medical University, Wenzhou, Zhejiang 325027, China*

Complete contact information is available at: https://pubs.acs.org/10.1021/acsomega.4c06294

https://doi.org/10.1021/acsomega.4c06294
ACS Omega 2024, 9, 43034−43045

Author Contributions

Conceptualization: W.-J.C. Data curation: W.-J.C., R.−R.C.; Z.-B.L.; J.L.. Formal analysis: W.-J.C., R.−R.C.; Z.-B.L.; J.L. Funding acquisition: R.Z. Investigation: R.Z. Methodology: W.-J.C. Project administration: R.Z. Resources: R.−R.C.; L.-J.H. Software: R.−R.C. Supervision: R.Z.. Validation: W.-J.C. Visualization: W.-J.Cai. Writing—original draft: W.-J.C.; R.−R.C.; Z.-B.L.; J.L., L.-J.H. Writing-review editing: W.-J.C.; R.Z.

Notes

The authors declare no competing financial interest.

There is no need for informed consent in our study since the unidentified data were free from medical ethics review.

Institutional review board approval and informed consent were not required in the current study because research data are publicly available and all patient data are deidentified.

■ ACKNOWLEDGMENTS

Not applicable

■ ABBREVIATIONS

UM:uveal melanoma
MMRGs:mitochondrial metabolism-related genes
MMI:MMRGs-derived index
LASSO:least absolute shrinkage and selection operator
TCGA:the cancer genome atlas
GDC:genomic data commons
GEO:gene expression omnibus
PCA:principal component analysis
GO:gene ontology
KEGG:Kyoto encyclopedia of genes and genomes
ROC:receiver operating characteristic
TMB:tumor mutation burden
OS:overall survival
AUC:area under the curve

■ REFERENCES

(1) Jager, M. J.; Shields, C. L.; Cebulla, C. M.; Abdel-Rahman, M. H.; Grossniklaus, H. E.; Stern, M. H.; Carvajal, R. D.; Belfort, R. N.; Jia, R.; Shields, J. A.; Damato, B. E. Uveal melanoma. *Nat. Rev. Dis. Primers* **2020**, *6* (1), No. 24.

(2) Singh, A. D.; Turell, M. E.; Topham, A. K. Uveal melanoma: trends in incidence, treatment, and survival. *Ophthalmology* **2011**, *118* (9), 1881−1885.

(3) Piperno-Neumann, S.; Piulats, J. M.; Goebeler, M.; Galloway, I.; Lugowska, I.; Becker, J. C.; Vihinen, P.; Van Calster, J.; Hadjistilianou, T.; Proença, R.; Caminal, J. M.; Rogasik, M.; Blay, J. Y.; Kapiteijn, E. Uveal Melanoma: A European Network to Face the Many Challenges of a Rare Cancer. *Cancers* **2019**, *11* (6), No. 817, DOI: 10.3390/cancers11060817.

(4) Banou, L.; Tsani, Z.; Arvanitogiannis, K.; Pavlaki, M.; Dastiridou, A.; Androudi, S. Radiotherapy in Uveal Melanoma: A Review of Ocular Complications. *Curr. Oncol.* **2023**, *30* (7), 6374−6396.

(5) Jackson, S. E.; Chester, J. D. Personalised cancer medicine. *Int. J. Cancer* **2015**, *137* (2), 262−266.

(6) Stålhammar, G.; Gill, V. T. The long-term prognosis of patients with untreated primary uveal melanoma: A systematic review and meta-analysis. *Crit. Rev. Oncol. Hematol.* **2022**, *172*, No. 103652.

(7) Slater, K.; Hoo, P. S.; Buckley, A. M.; Piulats, J. M.; Villanueva, A.; Portela, A.; Kennedy, B. N. Evaluation of oncogenic cysteinyl leukotriene receptor 2 as a therapeutic target for uveal melanoma. *Cancer Metastasis Rev.* **2018**, *37* (2−3), 335−345.

(8) Wu, Z.; Xiao, C.; Long, J.; Huang, W.; You, F.; Li, X. Mitochondrial dynamics and colorectal cancer biology: mechanisms and potential targets. *Cell Commun. Signaling* **2024**, *22* (1), No. 91.

(9) García-Miranda, A.; Montes-Alvarado, J. B.; Sarmiento-Salinas, F. L.; Vallejo-Ruiz, V.; Castañeda-Saucedo, E.; Navarro-Tito, N.; Maycotte, P. Regulation of mitochondrial metabolism by autophagy supports leptin-induced cell migration. *Sci. Rep.* **2024**, *14* (1), No. 1408.

(10) Shanmugasundaram, K.; Nayak, B. K.; Friedrichs, W. E.; Kaushik, D.; Rodriguez, R.; Block, K. NOX4 functions as a mitochondrial energetic sensor coupling cancer metabolic reprogramming to drug resistance. *Nat. Commun.* **2017**, *8* (1), No. 997.

(11) Jin, X.; Liu, D.; Kong, D.; Zhou, X.; Zheng, L.; Xu, C. Dissecting the alternation landscape of mitochondrial metabolism-related genes in lung adenocarcinoma and their latent mechanisms. *Aging* **2023**, *15* (12), 5482−5496.

(12) Meng, C.; Sun, Y.; Liu, G. Establishment of a prognostic model for ovarian cancer based on mitochondrial metabolism-related genes. *Front. Oncol.* **2023**, *13*, No. 1144430.

(13) Han, F.; Cao, D.; Zhu, X.; Shen, L.; Wu, J.; Chen, Y.; Xu, Y.; Xu, L.; Cheng, X.; Zhang, Y. Construction and validation of a prognostic model for hepatocellular carcinoma: Inflammatory ferroptosis and mitochondrial metabolism indicate a poor prognosis. *Front. Oncol.* **2022**, *12*, No. 972434.

(14) Wilkerson, M. D.; Hayes, D. N. ConsensusClusterPlus: a class discovery tool with confidence assessments and item tracking. *Bioinformatics* **2010**, *26* (12), 1572−1573.

(15) Engebretsen, S.; Bohlin, J. Statistical predictions with glmnet. *Clin. Epigenet.* **2019**, *11* (1), No. 123.

(16) Mayakonda, A.; Lin, D. C.; Assenov, Y.; Plass, C.; Koeffler, H. P. Maftools: efficient and comprehensive analysis of somatic variants in cancer. *Genome Res.* **2018**, *28* (11), 1747−1756.

(17) Zeng, D.; Ye, Z.; Shen, R.; Yu, G.; Wu, J.; Xiong, Y.; Zhou, R.; Qiu, W.; Huang, N.; Sun, L.; Li, X.; Bin, J.; Liao, Y.; Shi, M.; Liao, W. IOBR: Multi-Omics Immuno-Oncology Biological Research to Decode Tumor Microenvironment and Signatures. *Front. Immunol.* **2021**, *12*, No. 687975.

(18) Robinson, M. D.; McCarthy, D. J.; Smyth, G. K. edgeR: a Bioconductor package for differential expression analysis of digital gene expression data. *Bioinformatics* **2010**, *26* (1), 139−140.

(19) Wu, T.; Hu, E.; Xu, S.; Chen, M.; Guo, P.; Dai, Z.; Feng, T.; Zhou, L.; Tang, W.; Zhan, L.; Fu, X.; Liu, S.; Bo, X.; Yu, G. clusterProfiler 4.0: A universal enrichment tool for interpreting omics data. *Innovation* **2021**, *2* (3), No. 100141.

(20) Geeleher, P.; Cox, N.; Huang, R. S. pRRophetic: an R package for prediction of clinical chemotherapeutic response from tumor gene expression levels. *PLoS One* **2014**, *9* (9), No. e107468.

(21) Li, Q.; Yu, D.; Yu, Z.; Gao, Q.; Chen, R.; Zhou, L.; Wang, R.; Li, Y.; Qian, Y.; Zhao, J.; Rosell, R.; Tao, M.; Xie, Y.; Xu, C. TIPE3 promotes non-small cell lung cancer progression via the protein kinase B/extracellular signal-regulated kinase 1/2-glycogen synthase kinase 3β-β-catenin/Snail axis. *Transl. Lung Cancer Res.* **2021**, *10* (2), 936−954.

(22) Gu, Z.; Cui, X.; Sun, P.; Wang, X. Regulatory Roles of Tumor Necrosis Factor-α-Induced Protein 8 Like-Protein 2 in Inflammation, Immunity and Cancers: A Review. *Cancer Manage Res.* **2020**, *12*, 12735−12746.

(23) El-Baba, C.; Ayache, Z.; Goli, M.; Hayar, B.; Kawtharani, Z.; Pisano, C.; Kobeissy, F.; Mechref, Y.; Darwiche, N. The Antitumor Effect of the DNA Polymerase Alpha Inhibitor ST1926 in Glioblastoma: A Proteomics Approach. *Int. J. Mol. Sci.* **2023**, *24* (18), No. 14069, DOI: 10.3390/ijms241814069.

(24) Maillard, M.; Nishii, R.; Yang, W.; Hoshitsuki, K.; Chepyala, D.; Lee, S.; Nguyen, J. Q.; Relling, M. V.; Crews, K. R.; Leggas, M.; Singh, M.; Suang, J.; Yeoh, A.; Jeha, S.; Inaba, H.; Pui, C. H.; Karol, S. E.; Trehan, A.; Bhatia, P.; Antillon, K. F.; Bhojwani, D.; Haidar, C. E.; Yang, J. J. Additive effects of TPMT and NUDT15 on thiopurine toxicity in children with acute lymphoblastic leukemia across multiethnic populations. *J. Natl. Cancer Inst* **2024**, *116*, 702−710, DOI: 10.1093/jnci/djae004.

(25) Ceylan, D.; Karacicek, B.; Tufekci, K. U.; Aksahin, I. C.; Senol, S. H.; Genc, S. Mitochondrial DNA oxidation, methylation, and copy

https://doi.org/10.1021/acsomega.4c06294
ACS Omega 2024, 9, 43034−43045

number alterations in major and bipolar depression. *Front. Psychiatry* **2023**, *14*, No. 1304660.
(26) Wang, B.; Wang, M.; Lin, Y.; Zhao, J.; Gu, H.; Li, X. Circulating tumor DNA methylation: a promising clinical tool for cancer diagnosis and management *Clin. Chem. Lab Med.* 2024; Vol. *62*, 2111−2127, DOI: 10.1515/cclm-2023-1327.
(27) Sánchez-Vázquez, V. H.; Martínez-Martínez, E.; Gallegos-Gómez, M. L.; Arias, J. M.; Pallafacchina, G.; Rizzuto, R.; Guerrero-Hernández, A. Heterogeneity of the endoplasmic reticulum Ca(2+) store determines colocalization with mitochondria. *Cell Calcium* **2023**, *109*, No. 102688.
(28) Kuo, K. T.; Lin, C. H.; Wang, C. H.; Pikatan, N. W.; Yadav, V. K.; Fong, I. H.; Yeh, C. T.; Lee, W. H.; Huang, W. C. HNMT Upregulation Induces Cancer Stem Cell Formation and Confers Protection against Oxidative Stress through Interaction with HER2 in Non-Small-Cell Lung Cancer. *Int. J. Mol. Sci.* **2022**, *23* (3), No. 1663, DOI: 10.3390/ijms23031663.
(29) Liu, X.; Wang, F.; Fan, X.; Chen, M.; Xu, X.; Xu, Q.; Zhu, H.; Xu, A.; Pouladi, M. A.; Xu, X. CHCHD2 up-regulation in Huntington disease mediates a compensatory protective response against oxidative stress. *Cell Death Dis.* **2024**, *15* (2), No. 126.
(30) Lumibao, J. C.; Haak, P. L.; Kolossov, V. L.; Chen, J. E.; Stutchman, J.; Ruiz, A.; Sivaguru, M.; Sarkaria, J. N.; Harley, B.; Steelman, A. J.; Gaskins, H. R. CHCHD2 mediates glioblastoma cell proliferation, mitochondrial metabolism, hypoxia-induced invasion and therapeutic resistance. *Int. J. Oncol.* **2023**, *63* (5), No. 117, DOI: 10.3892/ijo.2023.5565.
(31) Vishwa, R.; BharathwajChetty, B.; Girisa, S.; Aswani, B. S.; Alqahtani, M. S.; Abbas, M.; Hegde, M.; Kunnumakkara, A. B. Lipid metabolism and its implications in tumor cell plasticity and drug resistance: what we learned thus far? *Cancer Metastasis Rev.* **2024**, *43*, 293−319, DOI: 10.1007/s10555-024-10170-1.
(32) Jin, Y.; Chen, M.; Penning, T. M. Rate of steroid double-bond reduction catalysed by the human steroid 5β-reductase (AKR1D1) is sensitive to steroid structure: implications for steroid metabolism and bile acid synthesis. *Biochem. J.* **2014**, *462* (1), 163−171.
(33) Zhu, P.; Feng, R.; Lu, X.; Liao, Y.; Du, Z.; Zhai, W.; Chen, K. Diagnostic and prognostic values of AKR1C3 and AKR1D1 in hepatocellular carcinoma. *Aging* **2021**, *13* (3), 4138−4156.
(34) Zhang, D.; Shi, R.; Xiang, W.; Kang, X.; Tang, B.; Li, C.; Gao, L.; Zhang, X.; Zhang, L.; Dai, R.; Miao, H. The Agpat4/LPA axis in colorectal cancer cells regulates antitumor responses via p38/p65 signaling in macrophages. *Signal Transduction Targeted Ther.* **2020**, *5* (1), No. 24.
(35) Coussens, L. M.; Werb, Z. Inflammation and cancer. *Nature* **2002**, *420* (6917), 860−867.
(36) Horii, M.; Matsushita, T. Regulatory B cells and T cell Regulation in Cancer. *J. Mol. Biol.* **2021**, *433* (1), No. 166685.
(37) Zhang, Y.; Zhang, Z. The history and advances in cancer immunotherapy: understanding the characteristics of tumor-infiltrating immune cells and their therapeutic implications. *Cell. Mol. Immunol.* **2020**, *17* (8), 807−821.

https://doi.org/10.1021/acsomega.4c06294
ACS Omega 2024, 9, 43034−43045